Electron Paramagnetic Resonance spectroscopy (EPR)

Simon Breitler, *Studiengang Chemie*, *5. Semester*, brsimon@student.ethz.ch
Matthias Geibel, *Studiengang Chemie*, *5. Semester*, mgeibel@student.ethz.ch
Daniel A. Frick, *Studiengang Chemie*, *5. Semester*, frickd@student.ethz.ch

Assistent: Dr. Inés Garcia Rubio

Team 4

Abstract:

The goal of this experiment was to familiarize ourselves with the electron paramagnetic resonance spectroscopy (EPR). The first part included an introduction on different methods to tune and calibrate the EPR using the samples Weak- and Strong-Pitch and DPPH, which were supplied by the manufacturer of the EPR spectrometer.
The second part was the examination of the hyper-fine coupling. As samples γ-irradiated quartz glass, phenalenyl radicals and $^{63}Cu(sal)_2$ in $Ni(sal)_2$ were used. The spectra were then simulated with the program "Simphonia" to get the appropriate Hamiltonians.

Zürich ZH, 11. October 2007

Simon Breitler Matthias Geibel Daniel A. Frick

1. Introduction

1.1. General information

When hearing magnetism-based spectroscopy, one is often and exclusively considering NMR as it is the most well-known technique in this field. Its much less known, but equally useful sibling, the Electron Paramagnetic Resonance (EPR) is mostly forgotten. This is unfortunate, since it offers superior performance, such as overall greater sensitivity in situations where NMR can't be considered effective. Furthermore, it can even be the only appropriate spectroscopic method, such as for radicals.
The difference between these techniques is the particle whose interaction with the magnetic field is measured. While in NMR the nucleus is used to describe its chemical surrounding, the particle of interest in EPR is the electron. The electrons coupling to a magnetic field (Zeeman Effect) has long been known, but only in the second half of the 20th century, the technology needed for the exploitation of this type of interaction has become available. The irritating radiation is in the microwave range in the area of GHz which is why relatively small magnetic fields are required.

1.2. Theory

The Zeeman-Effect

The interaction of an electron spin with a magnetic field B_0 can be described by the spin-Hamilton-operator

$$H_0 = g_e \beta_e B_0 = -\gamma_e \hbar B_0 S_z \quad [1]$$

and the energy eigenvalues

$$E\left(m_s = \frac{1}{2}\right) = \frac{1}{2} g_e \beta_e B_0 \quad [2]$$

$$E\left(m_s = -\frac{1}{2}\right) = -\frac{1}{2} g_e \beta_e B_0 \quad [3]$$

with the g-factor for the free electron g_e = 2.002319, the Bohr magneton β_e = 9.27402·10^{-24} J/T and the gyromagnetic ratio γ_e= –1.7608592.10^{11} s^{-1}T^{-1}.

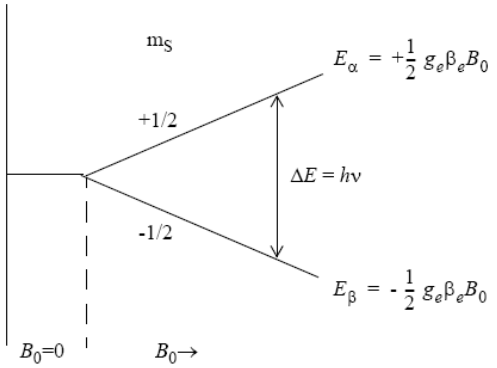

Figure 1: Schematic figure of the Zeeman energy splitting. (1)

Unlike conventional optical spectroscopy where a frequency sweep is done, i.e. the irradiated energy is changed, in EPR a range in the magnetic field is scanned. Due to limitations in microwave electronics, this procedure is easier and offers superior performance. The magnetic field strength where the splitting energy matches the irradiated energy is called "field for resonance". At this certain B_o a transition between the two spin states is induced.

The local surroundings of an unpaired electron causes a local magnetic field which is induced by the nucleus and the electrons. This induction changes the energy splitting of the Zeeman-effect. If other particles with a spin dissimilar to zero are in the surrounding, further splitting into more than just two peaks is observed.

Electron-Zeeman Interaction

The Hamiltonian for this interaction can be written as

$$H_{EZ} = g_e \beta_e B_{local} S_z = g_e \beta_e (1 - \sigma) B_o S_z. \quad [4]$$

The influence of the local field to the electron-Zeeman interaction is expressed by the g factor

$$g = (1 - \sigma) g_e \quad [5]$$

The g-factor gives information about the electronic structure of a paramagnetic compound. Additionally it can be used to identify radicals.

Hyperfine Interaction

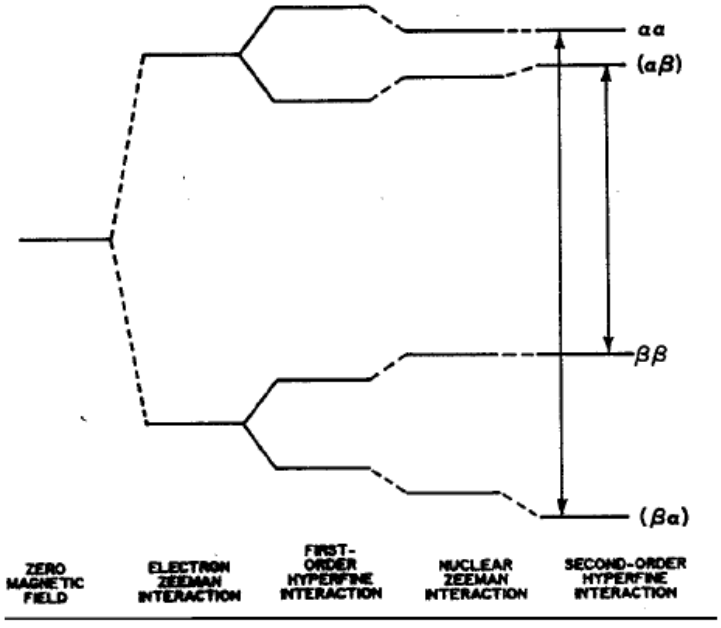

Figure 2: Schematic figure of four different Zeeman interactions. (1)

The additional magnetic field caused by the magnetic moment of the nucleus leads to a splitting of the EPR signal. The field for resonance is increased or lowered depending on the alignment of the magnetic moment of nearby particles.
In solution the isotropic parts of the interaction between electron and nuclear spin can be examined. The anisotropic part is compensated by the fast rotation of the compound in solution. For solids the anisotropic part of the interaction is predominant. For N nuclei with spin ½ one can observe 2^N EPR signals.

2. Experiment

2.1. Experimental setup

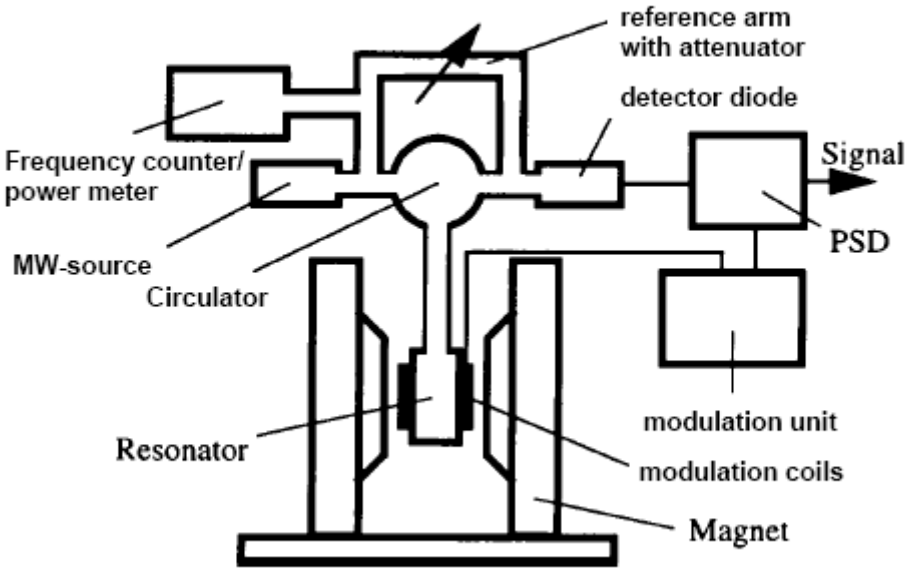

Figure 3: Scheme a CW (continuous-wave) EPR spectrometer. (1)

The experimental setup is presented in figure 3. The microwave-source produces a controlled electromagnetic wave excitation. The modulation and detection units are responsible for the amplification and the recording of the signal. The magnet unit provides the setup with a homogenous magnetic field in a well defined range. The resonator is capable of storing microwave energy and amplifying weak signals from the sample. The circulator controls the amount of microwaves that power goes the sample and from the sample back to the detector.

2.2. Execution of the experiment

The experiment was divided into four parts which will be explained separately.

2.2.1 EPR Basic

In the first part, the behavior of the signal in dependence of different experimental parameters was examined to find optimized conditions in order to get the best spectra. The following parameters were investigated: integration time, conversion time, receiver gain and the detection on first and second harmonics. “Strong pitch”, “weak pitch” and DPPH samples were used. With the data obtained the sensitivity of the spectrometer was determined.

2.2.2 EPR in solids

The second task was to measure the spectrum of γ-irradiated quartz glass. The spectrum was simulated with the program “Simphonia” afterwards.

2.2.3 Hyperfine interaction in liquids

The third part was the analysis of the hyperfine structure of phenalenyl radicals. First the spectrum was measured and then again simulated by the same software as in 2.2.2.

2.2.4 Transition metal complexes

The last part was the examination of a $^{63}Cu(sal)_2$-complex in $Ni(sal)_2$, followed by the simulation of the spectrum with the program "Simphonia".

3. Analysis and Results

3.1.1 EPR basics

The following influences of the parameters on the signal behavior have been observed:

Integration time (time constant): The time constant adjusts the responding time of the detector. The longer the time constant, the better is the ratio between noise and signal intensity. One has to take into account that with too long a time constant, the signal can be filtered out. Additionally the conversion time has to be longer than the time constant.

Conversion time: This parameter regulates the period of time in which a data point is integrated. A short period can lead to a loss of small signals. The effect of a long period is a better spectrum, but longer measurement times.

Receiver gain: The gain controls the amplification of the signal in the detecotr. If the adjustment is too high, the signal intensity is outside of detector's measuring range.

The following optimized parameters for the strong pitch were determined:

Microwave power:	1.008 mW	Integration time:	81.92 ms
Receiver gain:	60 dB	Conversion time:	163.84 ms
Field modulation:	1.00 G		

Tab 1. Strong Pitch Data (09.dat) for the Graph see Appendix A.8

3.1.2 "Weak Pitch" sample

The weak signal of the sample was optimized by variation of the different instrument parameters. The minimal number of detectable spins was calculated with following formula:

$$s = \frac{N_{spins}}{\Delta H_{pp}\sqrt{\Delta f}}\frac{1}{S/N} \qquad [6]$$

with the bandwidth of the phase sensitive detector $\Delta f = 1/2\pi$, the peak-to-peak line width ΔH_{pp} and the signal-to-noise ratio S/N. The result received from the "weak pitch" is s = 3.299 $10^{11}\sqrt{HzT}$.

3.1.3 Modulation amplitude for DPPH

The detection sensitivity is strongly increased by the field modulation. In case of a very strong modulation the signal was lost. The best DPPH-spectrum was received for a modulation amplitude of 20 G.

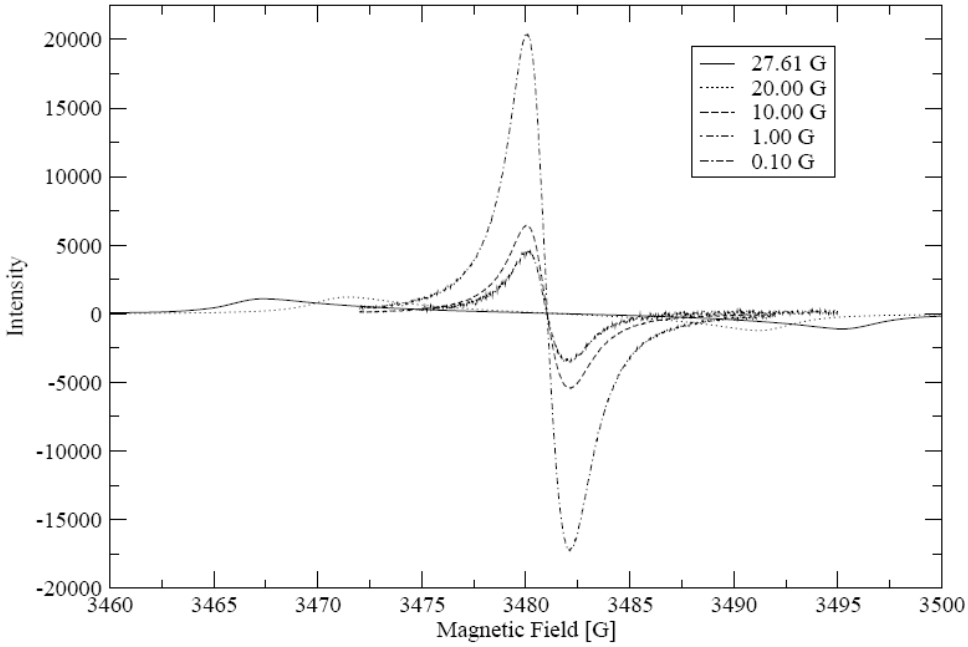

Figure 4: Measurement of DPPH with different modulation amplitudes.

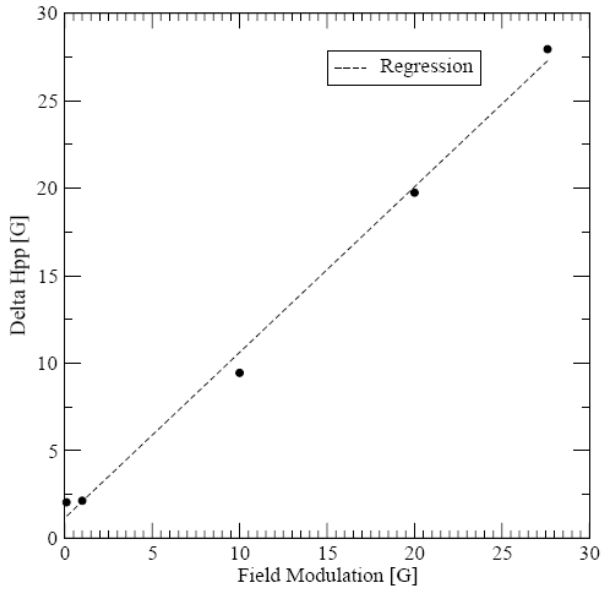

Figure 5: Plot of ΔH_{pp} versus the field modulation Amplitude (dots) and the performed linear regression (dotted line).

Figure 5 shows the linear relation between the field modulation and the peak-to-peak line width. The linear regression gives the following equation for the plot:

$$y = 1.1423 + 0.947 \cdot x. \qquad [7]$$

With the help of the measured spectrum the magnetic field was calibrated. The field of resonance is calculated by using following formula:

$$B = \frac{h\nu}{g\mu_B}. \qquad [8]$$

The g-factor was taken from the free electron with 2.0036. In comparison to the calculated value the experimental value shows a deviation of 4.5 Gauss of the magnetic field. The following data were calculated: B_{theo}: 3485.6 G, B_{exp}: 3481.1 G; for experimental data see appendix A.23.

3.2. EPR in solids

In the γ-irradiated quartz glass anisotropic effects are prevailing. The radiation transforms some SiO_4 tetrahedral to SiO_3 radicals whereby an axial g-tensor is created.

The plots and the simulated graph can be found in the Appendix section A.4.

3.3. Hyperfine interactions in liquids

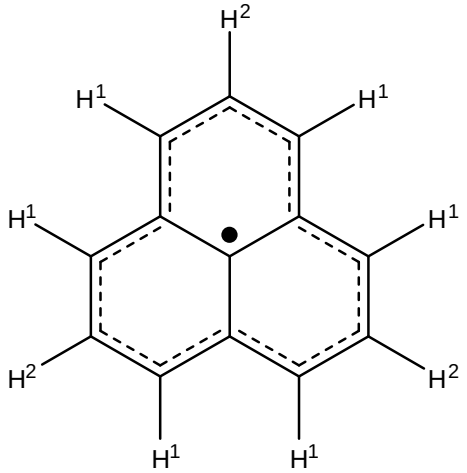

Figure 6: Structure of the phenalenyl radical.

The protons of the phenalenyl radical can be divided in two different classes of equivalent protons (H^1 and H^2 see figure 6) depending on their position in the molecule. There are two signals that split up in a quartet and a septet (see Appendix section A.5 Image A.26).

For the simulation the following data has been used:

Element	#	Isotope	spin	Iso. Abd.	g-factor	A[G]
H	3	1H	0.5	99.99	5.585	1.832
		2H	1	0.01	0.857	0
H	3	1H	0.5	99.99	5.585	1.832
		2H	1	0.01	0.857	0

Tab.2: Data for the simulation of the spectrum of phenalenyl radical.

The simulated spectrum can be found in the Appendix as figure A.26.

3.4. Transition metal complexes

The splitting of the signal is primarily caused by the spin interaction of the copper electron with the nitrogen nuclei which have a spin of 3/2. The coupling between and the oxygen isotope ^{17}O can be neglected since the isotopic abundance of ^{17}O is only about 0.038 % (5).

For the simulation the following data has been used:

Atom	**#**	**spin**	**A**	**Value [G]**
Cu	1	3/2	xx	40
			yy	40
			zz	200
N	2	1	xx	10
			yy	10
			zz	15

Tab.3: Data for the simulation of the spectrum of transition metal complex.

$g_x = 2.043$
$g_y = 2.043$
$g_z = 2.2$

The simulated spectrum can be found in the Appendix A.6.

4. Discussion

4.1 EPR basics

Using the Strong and Weak Pitch sample didn't provide any problems. After a few initial problems, the calibration of the continuous wave could be handled easily. Exploring the experimental settings gave sufficient background knowledge of the EPR spectrometer software.
Using the DPPH sample, which was provided for in the practicum, didn't work. The signal couldn't be observed even with different settings. After the preparation of a new sample the experiment could be conducted as described in the instruction provided by the assistant.

4.2 EPR in solid

The measurement of the first real spectrum didn't provide any problems. The measured spectrum was than used for the basic understanding of the for the simulation software. In contrast to the sample we measured before, the g-value was not isotropic anymore, but anisotropic. Therefore we had to find the appropriate g-values to simulate the spectrum.
Handling the program Simphonia was not exactly easy. A proper introduction on the simulation program was missing. The optimization of the simulated spectrum for the γ-irradiated gals was more a trial and error search than a funded, intuitive understanding of what was done.

4.3 Hyperfine structure in liquids

The measurement was not a problem, but unfortunately we missed some of the hyperfine structure on the first run. The scanning area where the B-field was varied was too small to see hyperfine-structure of the phenalenyl radical.
The understanding of the simulation was better understood, because an analogy between the EPR and the structure of the molecule could be drawn.

4.4 Transition Metal Complex

Measurement of the spectrum didn't cause any problem. The hyperfine-structure was difficult to understand and therefore difficult to simulate.

5. Appendix

5.1. Literature

(1) Experimental aspects of EPR, Prof. A. Angerhofer, http://www.esr.ethz.ch/, 11.10.2007.
(2) Complete script, Prof. A. Schweiger, http://www.esr.ethz.ch/, 11.10.2007.
(3) EPR lecture script, Gunnar Jeschke, http://www.mpip-mainz.mpg.de/~jeschke/, 11.10.2007.
(4) EPR theory, Prof. A. Angerhofer, http://www.esr.ethz.ch/, 11.10.2007.
(5) NuDat 2.4, http://www.nndc.bnl.gov/nudat2/, 11.10.07.